Acta Neuropathol (1992) 84: 484 – 494

Acta Neuropathologica

Immunotactoid-like endoneurial deposits in a patient with monoclonal gammopathy of undetermined significance and neuropathy

D. F. Moorhouse[1,2], R. I. Fox[3], and H. C. Powell[1]

Departments of [1]Pathology (Neuropathology) 0612, and [2]Anesthesiology, University of California San Diego and Veteran's Administration La Jolla, CA 92093, USA
[3]Department of Rheumatology, Scripps Clinic, La Jolla, CA 92093, USA

Received April 24, 1992/Accepted May 15, 1992

Summary. An 85-year-old man with a 2-year history of progressive lower limb weakness and paresthesia was found to have an IgG kappa monoclonal gammopathy of undetermined significance (mgus). Clinical and electrophysiological studies revealed a severe distal bilateral symmetrical polyneuropathy. A sural nerve biopsy showed extensive nerve fibre loss with the deposition of large amounts of amorphous material throughout the endoneurium. Electron microscopy showed the deposits to be composed of microtubular structures which were located diffusely throughout the endoneurium. The deposits were also located within the lumina of the vasa nervorum, some of which were undergoing disintegration and rupture with release of the proteinaceous material into the endoneurium. The regions of the nerve in which they appeared most numerous showed more severe nerve fibre damage than other areas. These microtubular structures were also observed in disintegrating vessels and adjacent endoneurium. On immunohistochemistry they stained with antibody to IgG. Identical deposits were found in the dermis in which there was a leucocytoclastic vasculitis. Located in linear arrays within the axons of myelinated and unmyelinated fibres were highly organised tubular structures resembling immunotactoids. Identification of immunotactoid-like structures within the nerve is unique and may be another mechanism by which monoclonal proteins can induce nerve fibre injury.

Key words: Neuropathy – Immunotactoid – Endoneurial deposits – Monoclonal gammopathy – Skin

Detection of monoclonal proteins in patients with neuropathy may lead to discovery of an underlying disease such as multiple myeloma [14], amyloidosis [18], Waldenstroms macroglobulinaemia [13], mgus [15] or lymphoma [36]. The exact relationship between the presence of these proteins within the serum and the development of a neuropathy is not fully resolved [6]. Numerous pathogenic mechanisms have been proposed to account for the neuropathy associated with monoclonal proteins including immunological [8, 9, 19, 21, 23, 27], ischaemic [7, 26], hyperviscosity [1]; and the effects of amyloidosis [3, 18], and physical compression of the nerve by the abnormal protein [7, 34, 37]. Direct visualisation of such large amounts of material within the endoneurium is unusual and has only been previously reported in a few cases [34, 35, 37].

Immunotactoid glomerulopathy is a recently recognised pathological entity [16, 29] characterised histologically by the deposition of organised microtubular structures within the mesangium and capillary basement membrane of the glomerulus. These structures, measuring between 12–49 nanometers in diameter [16], appear to be composed of immunoglobulin and complement and are larger than, and do not stain for, amyloid. The identification of these immunotactoid-like structures within the axons of myelinated and unmyelinated nerve fibres, together with the abnormal protein within the endoneurium may help to explain the development of the neuropathy in this patient with mgus.

Case report

An 85-year-old man first presented in 1989 with a 1-year history of progressive weakness, dysesthesias, and numbness in his lower limbs. He also had a rash involving his lower limbs and pain in his hands and feet without joint swelling. Neurological examination detected bilateral, symmetrical weakness and atrophy of the distal limb musculature, areflexia, and hypoesthesia for pin prick, light touch and temperature in a sock distribution. Vibration and proprioception were absent up to knee level. Upper limb examination revealed some mild, distal weakness and sensory loss involving his hands. Cranial nerves were normal.

Serum protein immunoelectrophoresis detected a monoclonal IgG kappa paraprotein. Quantitative immunoglobulin assay showed a slightly raised IgG at 1700 mg/100 ml (normal 723–1685 mg/100 ml) with normal levels of IgM and IgA. Electrophoresis of

Correspondence to: H. C. Powell (address see above)

the cerebrospinal fluid (CSF) detected a monoclonal IgG kappa band, routine analysis of the CSF including protein and glucose concentration and white cell count was normal. Complement studies revealed mild activation of complement with a Cd4/C4 ratio equal to 1.4 (normal = 0–1.1 vern units). Electromyography showed mild to moderate chronic denervation in the distal lower limb muscles; the proximal lower limb and upper limb muscles were normal. There was a small reduction in motor nerve conduction velocity in the lower and upper limbs, with the left median motor nerve conduction velocity = 44 m/s (normal = 49 m/s) and left peroneal nerve conduction velocity = 44 m/s (normal = 44–88 m/s). There were absent sensory nerve responses in the lower and upper limbs. The following laboratory investigations were normal: full blood count and differential, erythrocyte sedimentation rate, urea and electrolytes, urinalysis including examination for light chains, chest radiograph, full connective tissue screen, vitamin B12, CT of brain and thorax, skeletal bone survey, magnetic resonance imaging of cervical and thoraco-lumbar vertebrae, and a

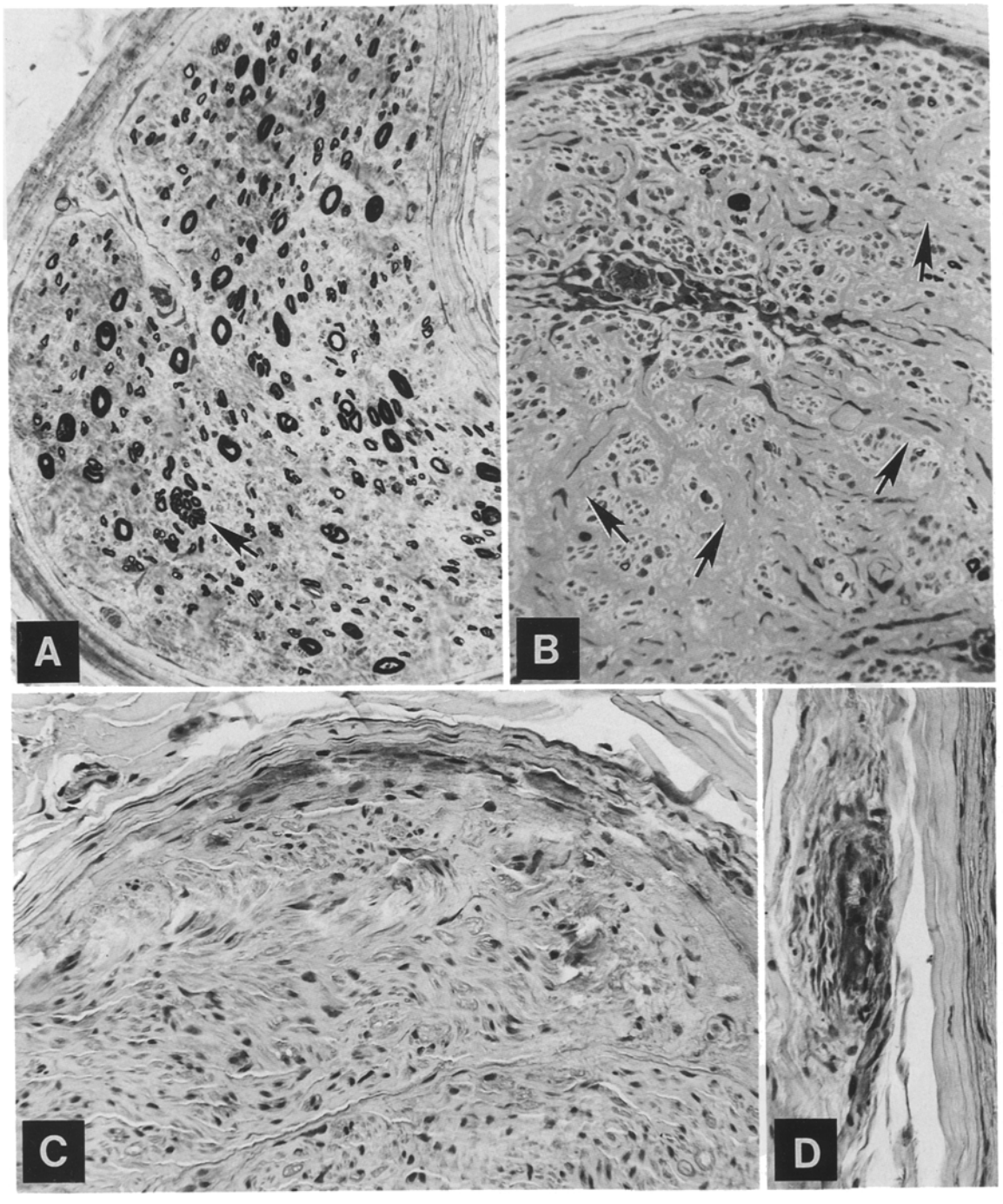

Fig. 1A–D. Light microscopic changes in the sural nerve biopsy. **A** Transverse section showing a generalised reduction in myelinated nerve fibres and many abnormally small and dystrophic fibres. A regenerating cluster is seen (*arrow*). ×310. **B** Transverse section from a fascicle showing amorphous proteinaceous deposits in the endoneurium (*arrow*). In contrast to **A** there is a paucity of myelinated fibres and no regenerating fibres are seen. Vessels are fewer than expected and are surrounded by endoneurial macrophages. Note the large number of macrophages in the subperineurial region. ×245. **C, D** Immunohistochemistry with antibody to IgG showing positive staining in the subperineurial region (**C**) and in an adjacent epineurial blood vessel (**D**). **C** ×295; **D** ×200

cryoglobulin screen. The clinical diagnosis at the time was a mixed sensory motor distal polyneuropathy.

Over the next 24 months his neuropathy progressively worsened; he was not able to walk unaided, and suffered from incapacitating painful dysesthesias involving both his upper and lower limbs. A 3-month course of oral steroids made no symptomatic or clinical improvement to the neuropathy. The results of electromyographic and nerve conduction studies showed further deterioration with evidence of acute and chronic denervation involving the upper limb muscles, and with motor nerve conduction velocity of the left median nerve was reduced to 29 m/s. There were no motor responses in his lower limbs. During this period, repeated radiographs and bone marrow aspirates for a plasma cell dyscrasia were negative. Two further tests for cryoglobulins were negative. Immunoelectrophoresis continued to detect a monoclonal IgG kappa band in the serum and CSF. He had two more acute attacks of the maculopapular skin rash which did not respond to the oral corticosteroids or to a course of dapsone. He developed severe flexion contractures of the hands and feet. Sural nerve and skin biopsies were performed.

Methods

A sural nerve biopsy was taken from just above the lateral malleolus and processed for light and electron microscopy. Material used for light microscopy was fixed in formalin, while tissue to be processed for electron microscopy and nerve fibre teasing was fixed in 2.5% phosphate-buffered glutaraldehyde and embedded in araladite resin. Myelinated fibre density and mean axonal size-frequency histograms were obtained using techniques previously described [5]. Immunohistochemistry was performed on paraffin sections using anti-IgG, anti-IgM and anti-IgA and anti-kappa and anti-lambda light chain sera. The plasma obtained by plasmapheresis was concentrated and processed for electron microscopy after using dialysis to produce a concentrated sample. A 4-mm punch biopsy was taken from the skin overlying the right knee, part of which was frozen for immunofluorescence studies, while the remaining tissue was placed in formalin and embedded in paraffin sections. The skin processed for electron microscopy was recovered from the paraffin-embedded sections.

Results

By light microscopy the nerve showed five medium-sized and three small fascicles with varying degrees of fibre loss. The epineurial and perineurial blood vessels were markedly thickened but there was no epineurial vasculitis. The number of endoneurial blood vessels appeared reduced. There was an extensive neuropathy with marked depletion of myelinated fibres, increased endoneurial connective tissue and accumulation of macrophages (Fig. 1A, B). Scattered throughout the endoneurium were large amounts of pale-staining, amorphous material which was most marked in the subperineurial region (Fig. 1B). This material did not stain with either congo red or thioflavin T. Immunohistochemistry showed extensive staining of the endoneurium to IgG which was most marked in the subperineurial region and around the vasa nervorum where the accumulation of the amorphous material was greatest (Fig. 1C, D). Axonal degeneration was widespread with no evidence of primary demyelination. Axon size-frequency histograms showed a loss of large- and medium-sized myelinated fibres, with many of the residual fibres 2–3 μm in diameter consistent with nerve regeneration. Myelinated fibre densities varied between those fascicles with and without deposits, 707/mm^2 to 5,744/mm^2 respectively, with an average value of 2,747/mm^2 (normal = 7,500–10,000/mm^2) [10]. Teased nerve fibre preparations did not show segmental demyelination.

By electron microscopy, the amorphous material throughout the endoneurium was composed of straight or slightly curved microtubular structures measuring between 100–300 nm in diameter (Fig. 2A, B). The tubular structures were most numerous in the subperineurial region where they seemed to be contained by the innermost layers of the perineurium. The endoneurial areas where the deposition of this material was greatest corresponded to the regions where the nerve fibre damage was most severe with extensive loss of myelinated fibres, increased connective tissue and numerous Bungner's bands (Fig. 3A). There was quite marked infiltration of macrophages most notable in the subperineurial region and also centered around the endoneurial blood vessels (Fig. 1B). Macrophages could be seen engulfing the tubular structures (Fig. 3A). In some instances, vascular profiles were observed with large amounts of the tubular material within the lumen and resting on the basal lamina (Fig. 4C–E). Vessels were fewer than expected in the endoneurium and showed a variety of reactive (Fig. 4A) and degenerative (Fig. 4B)

Fig. 2. Electron micrographs showing nerve (**A, B**) and skin (**C–E**). **A** The subperineurial space is filled by tubular electron-dense deposits, interspersed amongst which are islands of collagen fibrils. The deposits are contained by the inner layers of the perineurium and correspond to the amorphous, proteinaceous material observed in Fig. 1B. Note the absence of perineurial cells between opposing layers of redundant basal lamina. ×13,300. **B** High-power view of the subperineurial region showing transverse and longitudinal profiles of the tubular material which on transverse section can be seen to consist of single, bi- and trilayered tubules measuring 150–300 nm in diameter. The location of these deposits also corresponds to the antibody positivity by immunohistochemistry. A single collagen fibril can be identified in the center of the illustration. ×27,500. **C–E** Skin. **C** Electronmicrograph showing identical tubular material to that seen within the nerve present within the dermis. The tubular material appears to be forming from the edges of the electron-dense material in the dermis. ×20,000. *Inset:* The plasma precipitate has a fibrillary structure similar to the dermal deposit. ×10,400. **D** The tubular material can be seen forming at the edges of the electron-dense deposit. ×23,000. **E** High-power view of the tubular material in the dermis showing it to be identical to that seen within the nerve. ×32,500

Fig. 3. A A macrophage (*M*) can be seen engulfing the tubular structures some of which have been partially internalised (*arrow*). Tubular material which is in intracytoplasmic vacuoles (*V*) is less easily recognised. A large lipid droplet (*L*) is present within the cytoplasm of an unmyelinated fibre which also has immunotactoid-like material within its axons. All of the unmyelinated fibres in this field contain immunotactoid-like material. Situated in the center of this field is a Bungner's band (*B*) characterised by opposing Schwann cell surfaces enclosed by the basal lamina of a preexisting nerve fibre. ×24,000. **B** *Inset:* Dystrophic axon with tightly packed intraxonal organelles, reactive mitochondria and numerous lysosomes. ×5,600

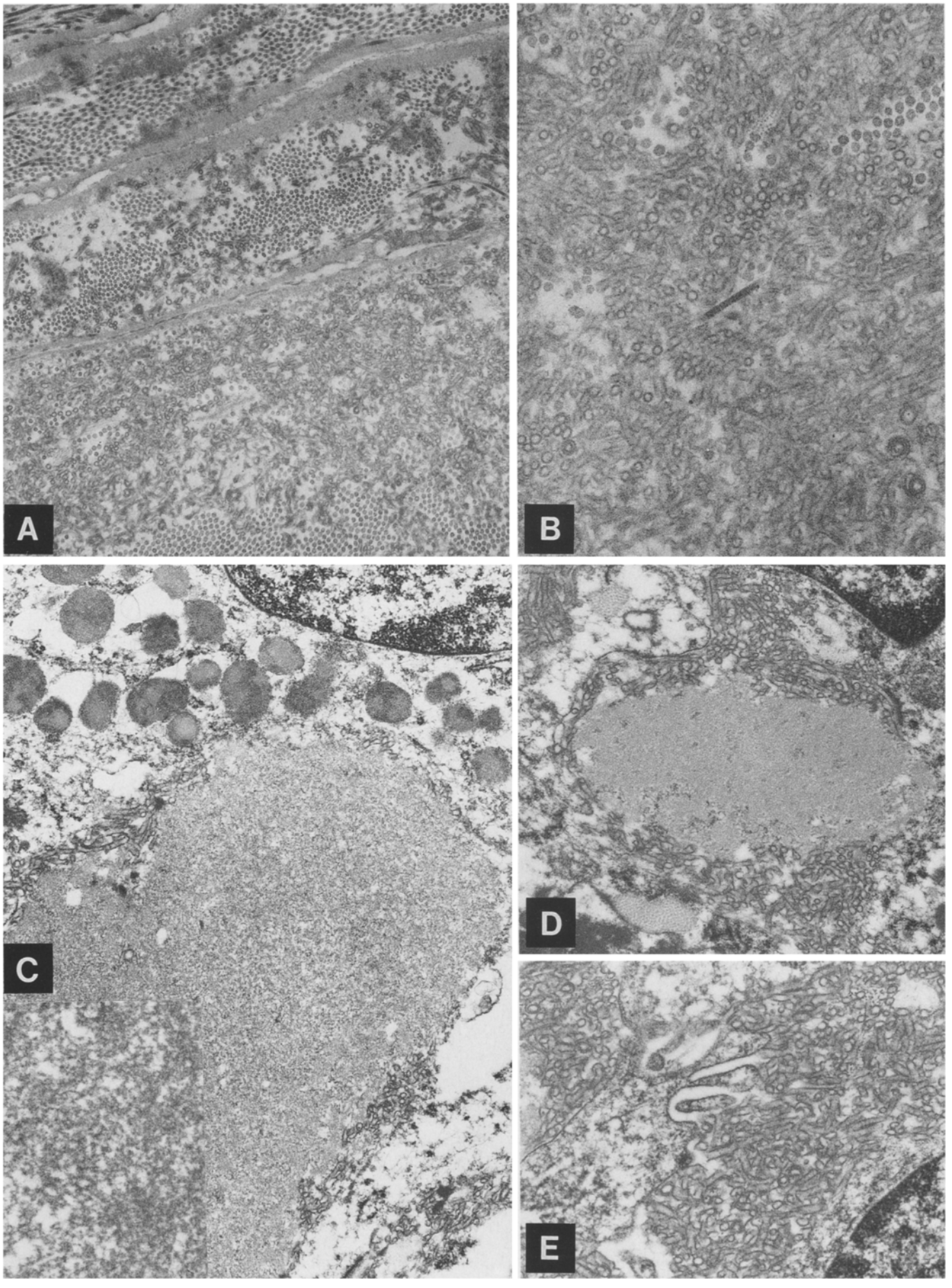

Fig. 2

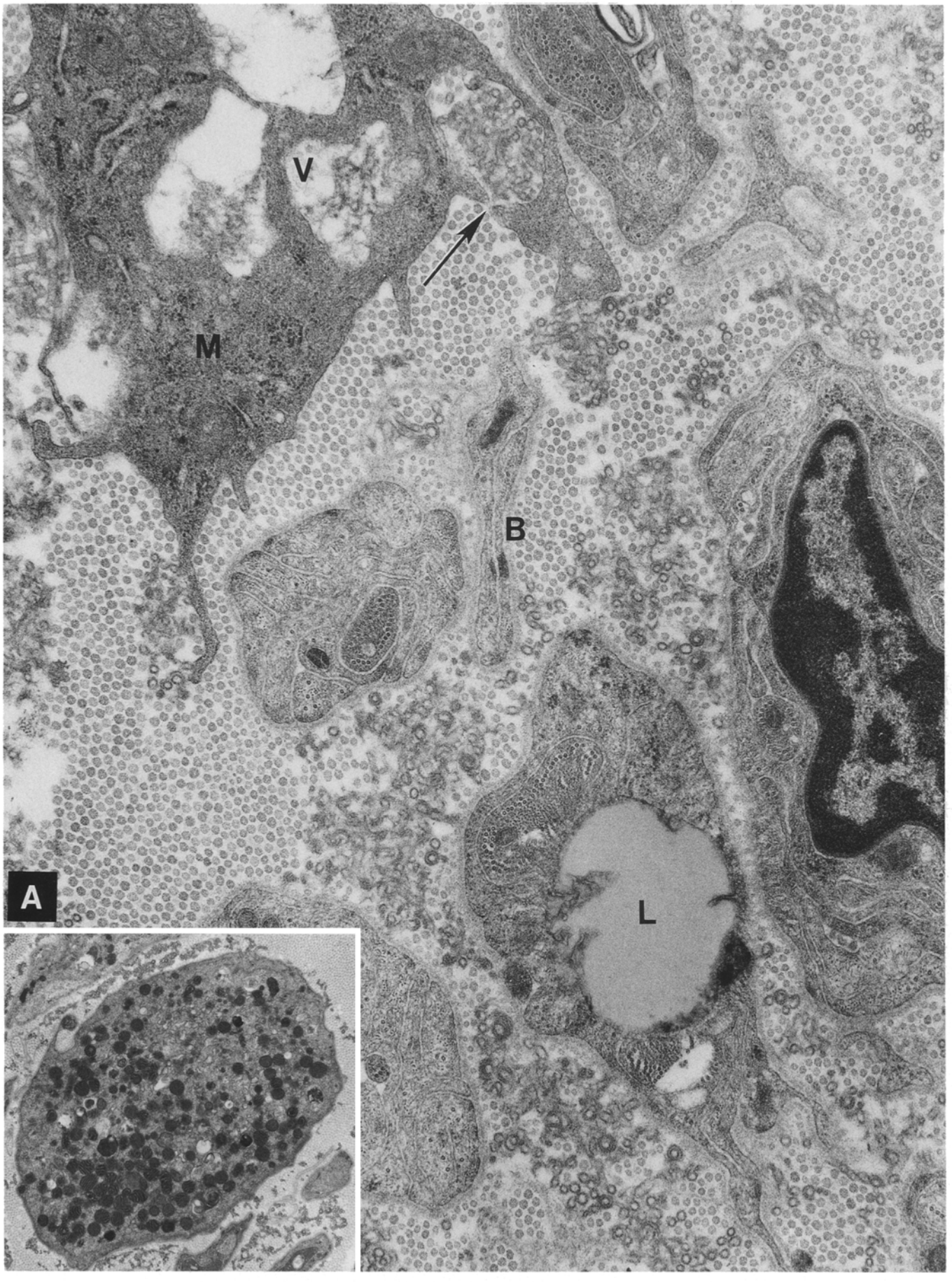

Fig. 3

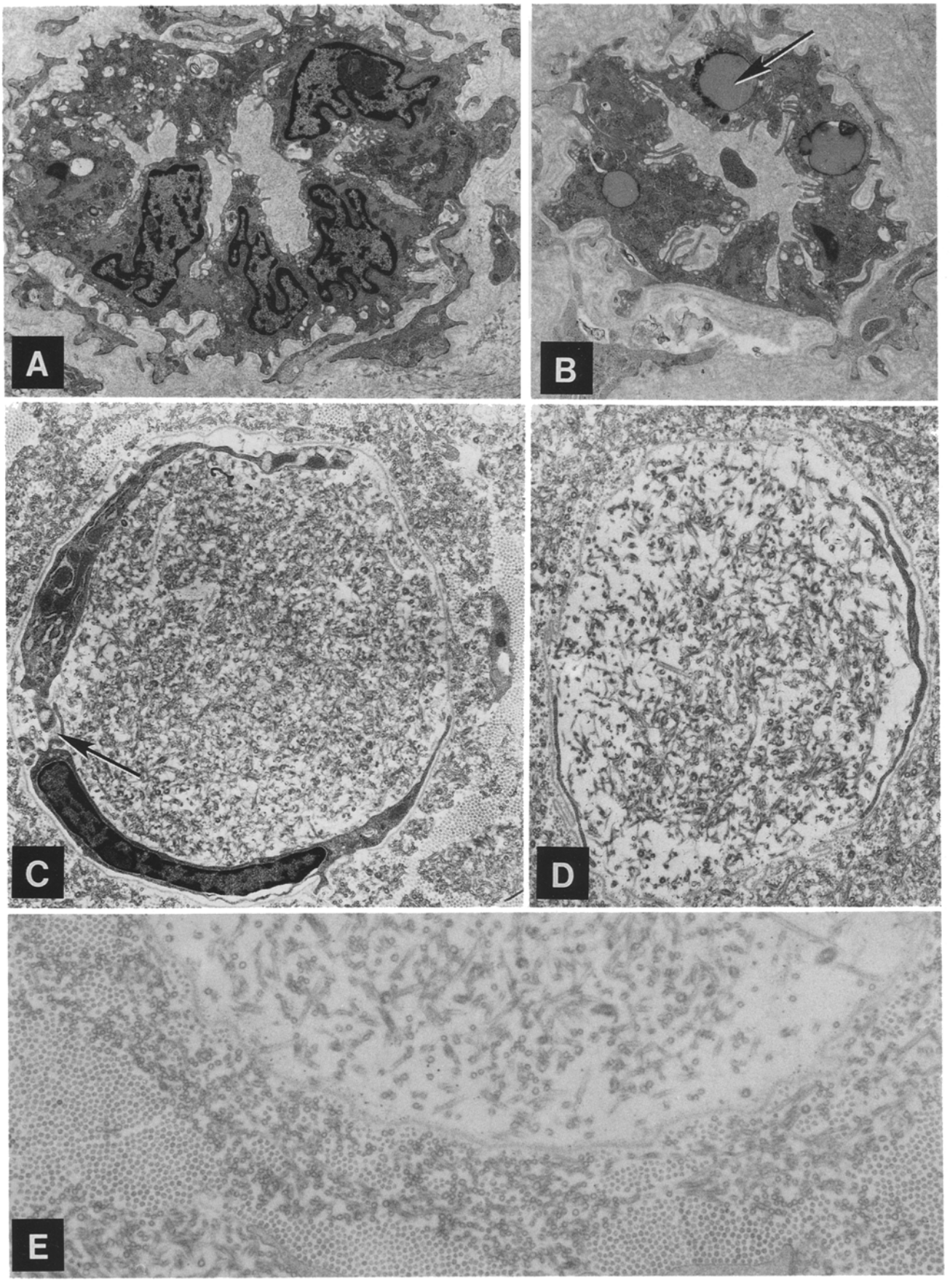

for legend see next page

changes. Microangiopathic changes included enlargement of endothelial cells (Fig. 4A) with accumulation of filaments and lipid inclusions (Fig. 4B). In some disintegrating vessels, large gaps appeared between endothelial cells, bringing the deposits into direct contact with basal lamina. The proteinaceous deposits were noted on either side of the basal lamina consistent with leakage into the interstitium (Fig. 4C–E). Arranged in linear arrays within the axons of myelinated and unmyelinated fibres were distinct tubular structures resembling immunotactoids, each having a central core and all measuring 40 nm in diameter (Fig. 5A). They were larger than microtubules and were not observed free within the endoneurium or within the walls or lumina of endoneurial capillaries. The myelinated fibres containing these structures showed axonal pathology with retraction of the axon away from an intact myelin sheath, and closely packed intra-axonal organelles (Fig. 5A). More severe damage was also seen with axonal degeneration and secondary collapse of the myelin sheath (Fig. 5A, inset). There was no evidence of demyelination or widened myelin lamellae.

The skin biopsy was diagnosed as leucocytoclastic vasculitis and showed an inflammatory process involving the dermal blood vessels and marked polymorphonuclear infiltration in the dermis especially around the dermal blood vessels. There was extensive staining with periodic acid-Schiff-positive material throughout the dermis. Immunofluorescence revealed extensive nonspecific staining of the skin with antibodies to IgG, IgA, IgM, complement and fibrinogen. By electron microscopy tubular profiles of identical dimensions to those observed in the endoneurium were also found in the dermis (Fig. 2C–E). These structures appeared in the dermal interstitium and were concentrated in perivascular areas which were also the site of inflammatory changes. No immunotactoid-like structures were seen within the biopsy. In some areas of the dermis there were large amounts of electron-dense material, from the edges of which the tubular structures appeared to be undergoing formation (Fig. 2C, D). Electron microscopy of the plasma revealed masses of material similar to the electron-dense material observed within the dermis and occasionally tubular material similar to that seen within the dermis and endoneurium (Fig. 2C inset).

Fig. 4A–E. Stepwise progression of the observed vascular injury. **A** A reactive vessel with marked endothelial cell enlargement. ×6,200. **B** Degenerating vessel with lipid inclusions (*arrow*) within the cytoplasm of the endothelial cells. The tubular proteinaceous material is seen surrounding this and the above vessel. ×7,500. **C** Endoneurial blood vessel with large amounts of the tubular material clearly visible within the lumen. The vessel is only partially lined by endothelium (no endothelium is seen in the *upper right hand* portion) and interendothelial tight junctions are absent (*arrow*). ×8,600. **D** A endoneurial vessel with vestigial remains of the endothelial cells and nearly complete exposure of the basal lamina. ×9,000. **E** Higher-power illustration of a portion of a vessel in which no endothelial lining was observed. Tubular material can be clearly seen within the lumen of this vessel and outside of the vessel in the adjacent endoneurial interstitium. ×16,000

Discussion

In this case, we describe unusual electron microscopic findings in a patient with an IgG kappa monoclonal gammopathy of undetermined significance (mgus), who has a neuropathy and a skin vasculitis. Clinically and electrophysiologically there were indications of a severe symmetrical polyneuropathy. This was confirmed histologically, with a marked reduction in myelinated fibre number, numerous dystrophic axons, and many axons which had retracted away from their myelin sheath. Immunotactoid-like structures were located within many of these axons (Fig. 5A). Fascicles containing the amorphous deposits and immunotactoid-like structures had fewer nerve fibres and vessels than adjacent fascicles in which the deposits were not observed (Fig. 1A, B). Extensive deposition of tubular proteinaceous material was identified within the endoneurium and dermis (Fig. 2A–E). This proteinaceous material appeared to be derived from the serum, as the masses of electron-dense proteinaceous material seen within the dermis had the same morphological appearance as that of the plasma precipitate and appeared similar to the material escaping from the damaged endoneurial blood vessels into the nerve interstitium. Interestingly, the tubular structures appeared to be forming from the edges of this material in the dermis (Fig. 2C, D). Immunohistochemically the tubular material was identified as IgG, or an IgG-related material. There was a marked reduction in the number of endoneurial blood vessels with many of the remaining vessels undergoing active disintegration and rupture, with release of the proteinaceous material directly from the blood into the endoneurium (Fig. 4C–E). Incidence of fibre damage appeared to correlate with the presence of immunotactoids (Fig. 5A) and vascular damage appeared to correlate with fibrillary tubular deposits in the endoneurium (Fig. 4A–E).

Direct ultrastructural demonstration of endoneurial immunoglobulin deposits is uncommon, and to date there have only been a few documented examples [27, 31, 34, 35, 37]. Extensive granulo-fibrillary endoneurial IgM deposits were seen by Yee et al. [37] in a case of mgus associated with mononeuritis multiplex. These deposits were scattered diffusely throughout the endoneurium and seemed to be contained by the inner layers of the perineurium. They suggested that compression of endoneurial capillaries by the large amounts of protein could lead to ischaemic damage and might be one of the factors contributing to the neuropathy. Endoneurial deposits in association with cryoglobulins have been

Fig. 5. A Abnormal nerve fibre with immunotactoid-like structures all measuring 40 nm in diameter arranged in a linear fashion inside the axon which is retracting away from its myelin sheath. The larger endoneurial tubular deposits can be seen surrounding the nerve fibre. ×32,000. **B, C** High-power view showing immunotactoid-like structures within the axons of unmyelinated fibres. Both fibres contain darkly staining mitochondria. **B** ×40,000; **C** ×55,400

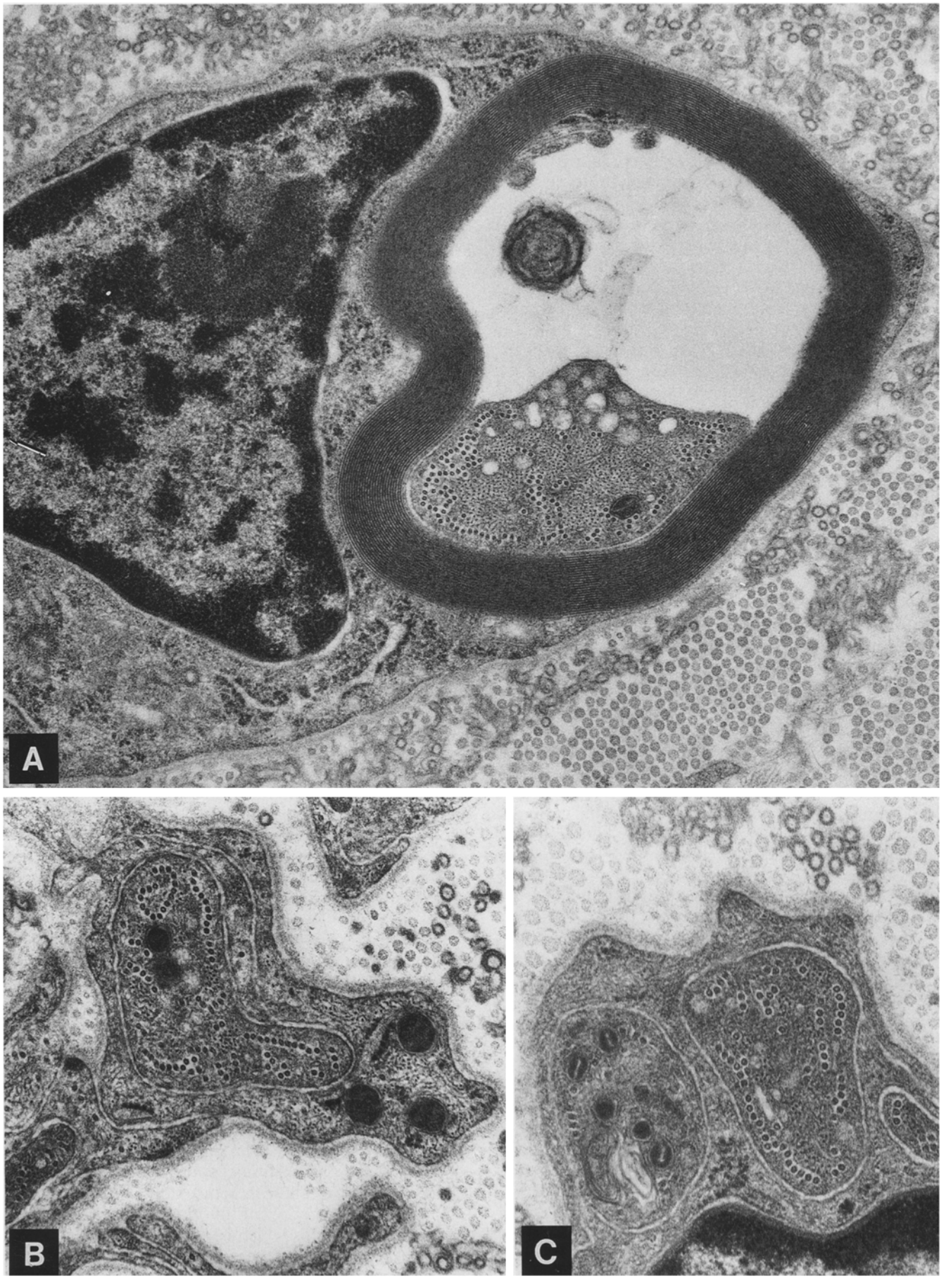
A
B
C

seen ultrastructurally on two occasions. Vallat et al. [34] noted microtubular, endoneurial deposits in a patient with an IgG kappa monoclonal protein, which were distributed diffusely throughout the endoneurium and within the walls and occasionally in lumina of the vasa nervorum. They proposed an ischaemic mechanism to the neuropathy as a result of monoclonal cryoglobulins occluding the vasa nervorum. In a nerve biopsy from a patient with a monoclonal IgM kappa cryoglobulin, Vital et al. [35] noted tubular endoneurial deposits measuring 50 nm in the walls of the vasa nervorum but not in the lumina. They noted, as we did, a direct correlation in fascicles between the amount of the proteinaceous deposit and the severity of the neuropathy. In this case, ultrastructural examination of the serum cryoprecipitate revealed a similar tubular structure to that seen within the endoneurium which suggested to them that the deposit was the circulating cryoglobulin. Sherman et al. [31] and Quattrini et al. [27] in their cases of neuropathy associated with monoclonal proteins both observed amorphous material scattered throughout the endoneurium; this material was of smaller dimensions than in our case or the cases mentioned above.

The specific mechanisms involved in the pathogenesis of our patient's neuropathy remains unclear. In the literature concerning abnormal deposition of protein in peripheral nerve two mechanisms are cited. Firstly, damage to vessels can occur, for example, in cases of familial amyloid polyneuropathy in which there is electron microscopic (EM) evidence of amyloid within the endoneurium [7], oedema and nerve fibre loss are present and ischaemia has been implicated in the pathogenesis of the neuropathy. Ischaemia, possibly contributing to neuropathy, could have been caused by a number of factors in our case; the observed endothelial cell proliferation, leading to narrowing of the lumina of the vasa nervorum, may impair nerve blood flow. Occlusion or narrowing of the lumina of the endoneurial capillaries could be caused by either external compression of the walls of the capillaries by the abnormal protein, or secondary to accumulation of the protein within the actual lumen. The observed reduction in the number of endoneurial capillaries and evidence of damage to the remaining vessels could result in ischaemia secondary to a reduction in endoneurial blood flow and may help explain cases of axonal neuropathy in which there are no antibody-mediated mechanisms. Secondly, in demyelinating neuropathies associated with monoclonal gammopathy, EM evidence of widened myelin lamellae precedes demyelination and complement consumption appears to play a critical part in the process [28]. Both these mechanisms have been proposed by other authors [7, 26, 34, 37] to explain the development of the neuropathy and may be relevant to this case.

In some previous cases with monoclonal proteins and neuropathy, immunological mechanisms have been proposed to account for the neuropathy [8, 9, 19, 21, 23, 27]. It has been shown for example that the monoclonal protein can bind to a carbohydrate determinant that is shared by myelin-associated glycoprotein (MAG) [21], and other glycolipids and glycoproteins [8] in peripheral nerve, leading to demyelination and/or widened myelin lamellae as a result of the protein binding to the myelin sheath. Recently, it has been demonstrated that in some patients with anti-MAG paraproteins the protein not only reacts with MAG but can also react with sulfatide, a major acidic glycoprotein of peripheral nerve myelin [9]. Furthermore, various paraproteins, including IgM and IgG, can bind to nerve constituents including chondroitin sulfate C and axonal proteins, and thereby possibly cause an axonal neuropathy by disruption of cellular processes such as axonal transport [11, 12, 23, 27, 31]. In one of these patients, the abnormal protein was IgG kappa as in our case. The authors demonstrated that the monoclonal protein bound to a low molecular weight neurofilament protein and suggested that this may have played a role in causing the axonal neuropathy [23]. The ultrastructural identification of immunotactoid-like structures within the axons of a patient with mgus and peripheral neuropathy is unique and may suggest another mechanism by which monoclonal proteins can induce nerve injury. These structures within the axons of myelinated and unmyelinated fibres could cause nerve fibre injury either by complement binding within the axon or, secondary to binding of various axonal constituents, disrupt axonal flow inducing axonal dystrophy and nerve fibre loss.

The term immunotactoid glomerulopathy has recently been introduced by Korbet et al. 1985 [16], to describe a distinct histological entity in renal pathology which was first reported by Rosenmann et al. in 1977 [29]. To date, approximately 60 cases have been reported [17]. By electron microscopy immunotactoid glomerulopathy is characterised by the non-random deposition within the glomerulus of highly organised ultrastructural microtubular deposits which appear to be composed predominately of immunoglobulin and complement. Korbet [16] used the term immunotactoid to describe these microtubular structures, stressing the organised orientation of the deposits and their immunoglobulin content. They may be of different lengths, depending on the degree of curvature, and their diameter is constant in each individual tissue sample but varies from case to case, with a range cited to be between 11 and 49 nm (mean value of 18–22 nm). The renal lesion is confined to the glomerulus in most examples, and its severity seems to be correlated with the amount of tactoidal material present within the glomerulus [16, 17]. The principal findings are mesangial cell thickening and thickening of the glomerular capillary basement membrane, which may be focal or diffuse. Staining for amyloid is negative in all cases. On immunofluorescence the principal finding is immunoglobulin deposition in a pattern that precisely reflects the distribution of the immunotactoids by electron microscopy.

Neither the exact physiochemical properties nor the precise reason why these structures form is known, but is thought to be the result of immune complexes or monoclonal proteins which have strong intermolecular attractions and that, in an appropriate osmotic environment, undergo tactoidal generation (i.e. abnormal pro-

tein crystallisation to form these microtubular structures) [16]. Flory [4] has shown that biopolymers randomly orientated in a liquid medium can evolve into an organised liquid crystal phase when the concentration of the medium is increased, such as may occur at the filtration surface of the kidney. However, as normal immunoglobulins under normal physiological conditions do not undergo tactoidal formation readily [32], it is possible that the immunoglobulins which do are abnormal in some way; for example, a monoclonal protein or a combination of immunoglobulin and complement (i.e. immune complexes). Why they developed within the nerve in our patient is unknown, but two of the variables which seem to be needed for immunotactoid formation, i.e. an abnormal protein and activation of complement, were present. It is conceivable that once the abnormal protein is within the axon it may combine with complement to form immunotactoids. The large amount of protein within the endoneurium and the unique microenvironment of peripheral nerve [22], which lacks lymphatic drainage, may have initiated osmotic changes leading to a favourable environment for tactoidal generation. The marked shrinkage of axoplasm noted in many of the fibres supports this possibility.

Initial reports of immunotactoid formation were limited to the kidney [16, 17]. However, with increased reporting of cases involving immunotactoids, questions arose as to whether they were in fact solely restricted to the kidney or part of a systemic disease process. In two previous accounts of immunotactoid glomerulopathy [24, 30], the patients also developed a leucocytoclastic skin vasculitis around the same time as they developed the renal pathology. No immunotactoids were identified in the skin biopsies on electron microscopy; however, in one instance large immune deposits were detected in and around small blood vessels in the skin. Both authors proposed that circulating immune complexes might be responsible for both disease processes, and the reason immunotactoids were identified within the kidney and not the skin in these patients is that crystallisation of immune deposits in both tissues is different. A recent case report documented immunotactoid formation within the alveolar-capillary interstitium of the lung and kidney in a patient suffering from renal failure and pulmonary haemorrhage [20]. That was the first time they were detected in an extrarenal location and the authors suggested that the identification of these structures within two different organs was possibly related to a circulating factor.

We now report their presence in a second extrarenal location (i.e. peripheral nerve). The possibility that the immunotactoid formation in this case is related to a circulating factor is likely, as it seems probable that they are derived from the large amounts of immunoglobulin within the endoneurium, which we have also identified within the dermis and the endoneurial blood vessels. The concurrent onset of the two disease processes (neuropathy, dermatitis), is also likely to be as a result of the circulating abnormal protein. Two courses of plasmapheresis led to a marked improvement in the patient's dermatological condition, which prior to this had failed to respond to oral medication. This success of plasmapheresis in refractory cutaneous vasculitis has been documented before [33]. Improvement in neurological symptoms would require plasmapheresis of longer duration [2] and in this case with advanced fibre damage (Fig. 1B) offers little prospect for substantial clinical improvement.

In previous electron micrographic studies [25] of paraproteinaemic neuropathy, endothelial proliferation and other microangiopathic changes have been described [26, 37], and damage to vessel walls can be inferred from observations of leakage of large molecular weight proteins into the endoneurium [34, 35, 37]. Our ultrastructural evidence of severe vascular damage secondary to the abnormal protein, leading to extravasation of this protein into the endoneurium, provides an unusual structural demonstration of the mechanism whereby the protein enters the endoneurium. This coupled with the unique identification of immunotactoid-like deposits within the nervous system may help to further explain mechanisms by which monoclonal gammopathies can lead to the development of neuropathies.

Acknowledgements. The authors are grateful to Robert S. Garrett, M. S., for excellent technical assistance.

References

1. Fahey JL, Barth WF, Solomon A (1965) Serum hyperviscosity syndrome. JAMA 192:464–467
2. Fineman SM, Kendall RR (1990) Plasma exchange: a treatment for neuropathy asociated with IgG kappa gammopathy. J Neurol 237:85–87
3. Fitting JW, Bischoff A, Regli F, De Grousaz G (1979) Neuropathy, amyloidosis, and monoclonal gammopathy. J Neurol Neurosurg Psychiatry 42:193–202
4. Flory PJ (1972) Molecular configurations and states of aggregation of biopolymers. Ciba Found Symp 7:109–124
5. Forcier NJ, Mizisin AP, Rimmer MA, Powell HC (1991) Cellular pathology of the nerve microenvironment in galactose intoxication. J Neuropathol Exp Neurol 50:235–255
6. Gossein S, Kyle RA, Dyck PJ (1991) Neuropathy associated with monoclonal gammopathies of undetermined significance. Ann Neurol 30:54–61
7. Hanyu N, Ikeda S, Nakadai A, Yanagisawa N, Powell HC (1989) Peripheral nerve pathological findings in familial amyloid polyneuropathy: a correlative study of proximal sciatic nerve and sural nerve lesions. Ann Neurol 25:340–350
8. Ilyas AA, Quarles RH, Dalakas MC, Brady RO (1985) Polyneuropathy with monoclonal gammopathy: glycolipids are frequently antigens for IgM paraproteins. Proc Natl Acad Sci USA 82:6697–6700
9. Ilyas AA, Cook SD, Dalakas MC, Mithen FA (1992) Anti-MAG IgM paraproteins from some patients with polyneuropathy associated with IgM paraproteinaemia also react with sulfatide. J Neuroimmunol 37:85–92
10. Jacobs JM, Love S (1985) Qualitative and quantitative morphology of the human sural nerve at different ages. Brain 108:897–924
11. Jakobsen J, Sidenius P, Braendgaard H (1986) A proposal for the classification of neuropathies according to their axonal transport abnormalities. J Neurol Neurosurg Psychiatry 49:986–990

12. Johnson KM, Conolly JA, Van der Kooy D (1986) Inhibition of axonal transport "in vivo" by a tubulin specific antibody. Brain Res 385:38–45
13. Julien J, Vital C, Vallat JM (1978) Polyneuropathy in Waldenstroms macroglobulinaemia. Arch Neurol 35:423–425
14. Kelly J, Kyle R, Myles JM, O'Brien PC, Dyck PJ (1981) The spectrum of peripheral neuropathy in multiple myeloma. Neurology 31:24–31
15. Kelly J, Kyle R, Myles JM, O'Brien PC, Dyck PJ (1981) Prevalence of monoclonal protein in peripheral neuropathy. Neurology 31:1480–1483
16. Korbet SM, Schwartz MM, Rosenburg BF, Sibley RK, Lewis EJ (1985) Immunotactoid Glomerulopathy. Medicine 64:228–243
17. Korbet SM, Schwartz MM, Lewis EJ (1991) Immunotactoid Glomerulopathy. Am J Kidney Dis 27:247–257
18. Kyle RA, Greipp PR (1983) Amyloidosis: clinical and laboratory features in 229 cases. Mayo Clin Proc 58:665–683
19. Latov N, Hays AP, Sherman WH (1988) Peripheral neuropathy and anti-MAG antibodies. CRC Crit Rev Neurobiol 3:301–332
20. Masson RG, Rennke HG, Gottlieb MN (1992) Pulmonary haemorrhage in a patient with fibrillary glomerulonephritis. N Engl J Med 326:36–40
21. Mendell JR, Sahenk Z, Whitaker JN, Trapp BD, Yates AJ, Griggs RC, Quarles RH (1985) Polyneuropathy and IgM monoclonal gammopathy: studies on the pathogenic role of anti-myelin associated glycoprotein antibody. Ann Neurol 17:243–254
22. Mizisin AP, Kalichman MW, Myers RR, Powell HC (1991) Role of the blood-nerve barrier in experimental nerve edema. Toxicol Pathol 8:170–185
23. Nemni R, Feltri ML, Fazio R, Quattrini A, Lorenzetti I, Corbo M, Canal N (1990) Axonal neuropathy with monoclonal IgG kappa that binds to a neurofilament protein. Ann Neurol 28:361–364
24. Orifila C, Meeus F, Bernadet P, Lepert J-C, Sue J-M (1991) Immunotactoid glomerulopathy and cutaneous vasculitis. Am J Nephrol 11:67–72
25. Podell DN, Packman CH, Maniloff J, Abraham GN (1987) Characterisation of monoclonal IgG cryoglobulins: fine structural and morphological analysis. Blood 69:677–681
26. Powell HC, Rodriguez M, Hughes RAC (1984) Microangiopathy of the vasa nervorum in dysglobulinaemic neuropathy. Ann Neurol 15:386–394
27. Quattrini A, Nemni R, Fazio R, Iannoccone S, Lorenzetti I, Grassi F, Canal N (1991) Axonal neuropathy in a patient with monoclonal IgM reactive with Schmidt-Lantermann incisures. J Neuroimmunol 33:73–79
28. Raine CS, Diaz M, Pakingan M, Bornstein MB (1979) Antiserum induced dissociation of myelinogenesis in vitro: an ultrastructural study. Lab Invest 38:397–403
29. Rosenmann E, Eliakim M (1977) Nephrotic syndrome associated with amyloid-like glomerular deposits. Nephron 18:301–308
30. Schifferli JA, Merot Y, Cruchard A, Chalelanat F (1987) Immunotactoid glomerulopathy with leucocytoclastic skin vasculitis and hypocomplementaemia: a case report. Clin Nephrol 27:151–155
31. Sherman WH, Latov N, Hays AP, Takatsu M, Nemni R, Galassi G, Osserman EF (1983) Monoclonal IgMκ antibody precipitating with chondroitin sulfate C from patients with axonal polyneuropathy and epidermolysis. Neurology 33:192–201
32. Steiner LA, Lopes AW (1979) The crystalisable human myeloma protein Dob has a hinge-region deletion. Biochemistry 18:4054–4067
33. Turner AN, Whittaker S, Banks I, Russell Jones R, Pusey CD (1990) Plasma exchange in refractory cutaneous vasculitis. Br J Dermatol 122:411–415
34. Vallat JM, Desproges-Gotteron R, Leboutet MJ, Loubet A, Gualde N, Treves R (1980) Cryoglobulinaemic neuropathy: a pathological study. Ann Neurol 8:179–185
35. Vital A, Vital C, Ragnaud JM, Baquey A, Aubertin J (1991) IgM cryoglobulin deposits in the peripheral nerve. Virchows Arch [A] 418:83–85
36. Walsh JC (1971) Neuropathy associated with lymphoma. J Neurol Neurosurg Psychiatry 34:42–50
37. Yee WC, Hahn AF, Hearn SA, Rupar AR (1989) Neuropathy in IgM paraproteinaemia. Acta Neuropathol 78:57–64